Dynamic Behaviour of Cantilever Bridges under Moving Loads

Le comportement dynamique de ponts en poutres articulées sous l'influence de charges mouvantes

Das dynamische Verhalten von Gerberträgerbrücken unter bewegten Lasten

N. NAGARAJU

Assistant Professor of Civil Engineering, Pant College of Tchnology, Paentnagar, India

K. S. JAGADISH

Lecturer in Civil Engineering, Indian Institute of Science, Bangalore, India

K. T. SUNDARA RAJA IYENGAR

Professor of Civil Engineering, Indian Institute of Science, Bangalore, India

1. Introduction

The vibration of highway bridges under the passage of heavy vehicles has been the subject of many investigations in recent years. The advent of faster and heavier highway vehicles and the modern tendency to design bridges with large span-to-depth ratios have enhanced the necessity of studying the dynamics of highway bridges.

The bridge-vehicle motion is complicated due to the numerous variables involved and the difficulty in incorporating them into the analysis. The major variables influencing the response are: the vehicle speed, the frequency and mass ratios, damping in the bridge and the vehicle, initial oscillation of the vehicle and unevenness of the bridge deck. It is difficult to consider all these variables at once.

Many investigations have been carried out idealizing the bridge as a beam; in a few cases it is also treated as a two-dimensional system [1, 2, 3, 4]. The vehicle is represented by a moving constant force or a combination of sprung and unsprung masses.

OEHLER [5] has been one of the early investigators in the field of bridge vibration. He conducted field tests on bridges of different types; simple-span, continuous, and cantilever type. His conclusions indicate that the cantilever bridges are the most susceptible to large amplitudes and longer duration of vibration than the other types.

KONISHI and KOMATSU [6] have derived the mathematical equations for a cantilever bridge, but they have not obtained numerical results. HUANG and VELETSOS [7] have made an analytical study of the problem referring to one fixed set of aspect ratios.

WEN and TORIDIS [8] carried out a more detailed investigation of the frequency analysis and the dynamic response of symmetrical double cantilever bridges. They idealized the bridge as a lumped mass system with five mass concentrations and represented the vehicle by a moving constant force. Numerical results are presented for bridges of various aspect ratios and various values of the speed parameter. They have noted in their conclusion the great susceptibility of cantilever bridges to vibration, the importance of higher modes, and the influence of the variation of speed parameter on the dynamic response.

JAGADISH and PAHWA [9] conducted the frequency analysis of a double cantilever bridge treating it as a distributed mass system. Covering a wide range of aspect ratios, their results indicate that the frequency-spectrum for a cantilever bridge is dense in contrast with that for a simply supported beam. The higher modes, it is pointed out, may have significant influence on the bridge response.

VELETSOS and HUANG [10] reported an analysis of the dynamic response of cantilever bridges. They considered the bridge as a multi-degree-of-freedom linearly elastic system having distributed flexibility and concentrated point masses, and the vehicle as a three-axle sprung load unit taking into account the effect of interleaf friction in its suspension system. They have presented the response histories for a three-span cantilever bridge with suspended side spans when a single-axle sprung load moves on the bridge. They have concluded that the cantilever bridges are the most susceptible to vibrations followed by simple-span bridges and then continuous bridges. The effects of the interaction force between the moving load and the bridge and the initial oscillation of the vehicle are discussed.

The present study pertains to the dynamic behaviour of double cantilever bridges under moving vehicles. There are a number of cantilever bridges in northern part of India and failures in a few cases [11] have been reported. It was therefore thought desirable to investigate such structures under dynamic loading.

In order to simplify the problem to its bare essentials, leading to a gross understanding of the behaviour of the structure, the bridge and the vehicle are approximated by simple models.

The Bridge Model

The bridge is treated as a continuous system by assuming it as a beam of uniform flexural rigidity EI and mass per unit length γ. This beam idealiza-

tion of the bridge implies that the deflection configuration along a transverse section is constant. The effects of shear deformation and rotatory inertia are neglected. The assumption of the bridge as a single beam gives fairly accurate results if the bridge is relatively narrow and the vehicle is positioned along the centre line. Damping is neglected as it is observed to be small in highway bridges, being of the order of 1 to 3% of the critical [12].

The Vehicle Model

Two simple models are used to represent the vehicle: (I) a moving constant force, and (II) a moving sprung load. Detailed numerical results are presented for four bridges of different aspect ratios for the moving force problem and for a few typical cases in the moving sprung load problem.

2. Cantilever Bridge under Moving Force

The moving force model ignores the dynamic characteristics of the vehicle. However earlier investigations [13] using beam theory have shown that this representation is useful when the vehicle frequency is small in comparison with the fundamental frequency of the bridge.

2.1. Analysis

A symmetrical double cantilever bridge under the action of a moving force is shown in Fig. 1. The two ends M and R of the bridge are simple supports; O and P are the two hinges. OP is the central suspended span. P is the moving force which is assumed to move from left to right with a constant velocity v.

Ignoring damping, the equation of motion of the bridge under the moving force may be written as

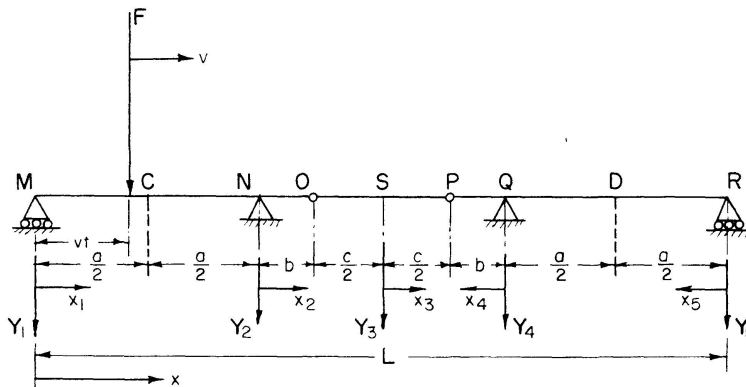$$EI\frac{\partial^4 Y}{\partial x^4} + \gamma\frac{\partial^2 Y}{\partial t^2} = F\delta(x - vt). \tag{1}$$

Fig. 1. Cantilever bridge under moving force.

The solution $Y(x, t)$ of Eq. (1) can be expanded in terms of the normal coordinates of the beam.

Let
$$Y(x, t) = \sum_{n=1}^{\infty} A_n(t) \phi_n(x). \tag{2}$$

$A_n(t)$'s represent the normal coordinates; $\phi_n(x)$ is the characteristic shape and is defined in Table A.

The right hand side of (1) can be expanded as

$$F \delta(x - v t) = \sum_{n=1}^{\infty} B_n(t) \phi_n(x). \tag{3}$$

Let
$$\int_0^L \phi_n^2(x) \, dx = K_n L. \tag{4}$$

Using (2), (3), and (4) in (1),

$$E I A_n(t) \phi_n^{IV}(x) + \gamma \ddot{A}_n(t) \phi_n(x) = \frac{F \phi_n(v t)}{K_n L} \phi_n(x). \tag{5}$$

Using the relations

$$\phi_n^{IV}(x) = \frac{\lambda_n^4}{c^4} \phi_n(x), \tag{6a}$$

and
$$\lambda_n^4 = \frac{\gamma \omega_n^2}{E I} c^4, \tag{6b}$$

in (5) and simplyfing,

$$\ddot{A}_n(t) + \omega_n^2 A_n(t) = \zeta_n \phi_n(v t), \tag{7}$$

where
$$\zeta_n = \frac{F}{\gamma L K_n}.$$

ω_n is the circular frequency of vibration of the bridge in the nth mode.

Taking Laplace Transforms on both sides of (7) and incorporating the initial conditions $A_n(0)$ and $\dot{A}_n(0)$ the expression for $A_n(t)$ reduces to

$$A_n(t) = A_{n0} \cos \omega_n t + \frac{\dot{A}_{n0}}{\omega_n} \sin \omega_n t + \zeta_n L^{-1} \left[\frac{1}{s^2 + \omega_n^2} L \phi_n(v t) \right]. \tag{8}$$

$\phi_n(v t)$ is now computed for each span and $A_n(t)$ is determined by substituting appropriate values for A_{n0} and $\dot{A}_{n0}$. A_{n0} and $\dot{A}_{n0}$ are both assumed to be zero for the first span $M N$. For subsequent spans they are determined by substituting proper values of t in the expressions for $A_n(t)$ and $\dot{A}_n(t)$ respectively.

Table A. Definition of $\phi_n(x)$

$$\phi_{nj}(x_j) = A_{nj}\cos\frac{\lambda_n x_j}{c} + B_{nj}\sin\frac{\lambda_n x_j}{c} + C_{nj}\cosh\frac{\lambda_n x_j}{c} + D_{nj}\sinh\frac{\lambda_n x_j}{c};$$

nth mode, jth Span
$n = 1, 2, 3, 4 \ldots$
$j = 1, 2, 3, 4, 5 \ldots$

Span No. (j)	Origin for x_j	Origin for t_j	x_j as a Function of t_j	t_j as a Function of t	Relation between x and x_j	Expression for $\phi_n(x)$	
1	M	M	$x_1 = vt_1$	$t_1 = t$	$x_1 = x$	$\phi_n(x) = \phi_{n1}(x_1)$	$x_1 = x$
2	N	N	$x_2 = vt_2$	$t_2 = t - \dfrac{a}{v}$	$x_2 = (x-a)$	$\phi_n(x) = \phi_{n2}(x_2)$	$x_2 = x-a$
3	S	O	$x_3 = \left(vt_3 - \dfrac{c}{2}\right)$	$t_3 = \left(t - \dfrac{a+b}{v}\right)$	$x_3 = x - \left(a+b+\dfrac{c}{2}\right)$	$\phi_n(x) = \phi_{n3}(x_3)$	$x_3 = x - \left(a+b+\dfrac{c}{2}\right)$
4	Q	P	$x_4 = (b - vt_4)$	$t_4 = \left(t - \dfrac{a+b+c}{v}\right)$	$x_4 = (a+2b+c-x)$	$\phi_n(x) = \phi_{n4}(x_4)$	$x_4 = (a+2b+c-x)$
5	R	Q	$x_5 = (a - vt_5)$	$t_5 = \left(t - \dfrac{a+2b+c}{v}\right)$	$x_5 = (2a+2b+c-x)$ or $(L-x)$	$\phi_n(x) = \phi_{n5}(x_5)$	$x_5 = (2a+2b+c-x)$ or $(L-x)$

2.2. Deflection and Moment

Deflection

The deflection $Y(x, t)$ is given by

$$Y(x, t) = \sum_{n=1}^{\infty} A_n(t) \phi_n(x). \tag{2}$$

Therefore

$$M(x, t) = -EI \frac{\partial^2 Y}{\partial x^2} = \sum_{n=1}^{\infty} A_n(t) \phi_n''(x), \tag{9}$$

where $M(x, t)$ represents the bending moment.

Once $A_n(t)$ and $\phi_n(x)$ are known, the response calculation is straightforward; one has only to substitute these quantities in (2) and (9), and obtain the result. The only precaution necessary is that sufficient number of terms on the righthand sides of (2) and (9) must be taken, if the two series converge rapidly, a few terms would suffice. In this case, the differentiated series (9) is not found to converge satisfactorily. It is therefore convenient to split up the response $Y(x, t)$ into two parts:

$$Y(x, t) = V(x, t) + U(x, t). \tag{10}$$

$V(x, t)$ satisfies the differential equation

$$EI \frac{\partial^4 V}{\partial x^4} = F \delta(x - vt) \tag{11}$$

and is termed as the "Quasi-static Solution". $U(x, t)$ is the reponse due to "Inertia Forces" and is referred to as the "Inertia Force Solution".

$V(x, t)$ is obtained by a static analysis of structure avoiding series summation. The inertia forces are well distributed over the structure; hence the computation of $U(x, t)$ is accomplished without much difficulty.

Differentiating (10) with respect to t and x separately and using in (1),

$$EI \frac{\partial^4 V}{\partial x^4} + EI \frac{\partial^4 U}{\partial x^4} + \gamma \frac{\partial^2 V}{\partial t^2} + \gamma \frac{\partial^2 U}{\partial t^2} = F \delta(x - vt). \tag{12}$$

Substituting for $EI \frac{\partial^4 V}{\partial x^4}$ from (11) and simplifying

$$EI \frac{\partial^4 U}{\partial x^4} = -\gamma \left(\frac{\partial^2 V}{\partial t^2} + \frac{\partial^2 U}{\partial t^2} \right) = -\gamma \frac{\partial^2 Y}{\partial t^2}. \tag{13}$$

Differentiating (2) with respect to t and substituting for the right hand side of (13),

$$EI \frac{\partial^4 U}{\partial x^4} = -\gamma \sum_{n=1}^{\infty} \ddot{A}_n(t) \phi_n(x). \tag{14}$$

$U(x, t)$ is now expanded in a series of the characteristic function of the bridge as

$$U(x, t) = \sum_{n=1}^{\infty} a_n(t) \phi_n(x). \tag{15}$$

From (13), (15) and (2), it can be shown that

$$a_n(t) = -\frac{\gamma c^4}{EI} \frac{1}{\lambda_n^4} \ddot{A}_n(t). \tag{16}$$

Hence
$$U(x,t) = -\frac{\gamma c^4}{EI} \sum_{n=1}^{\infty} \frac{1}{\lambda_n^4} \ddot{A}_n(t) \phi_n(x). \tag{17}$$

$V(x,t)$, by the elementary theory of bending of beams, can be written as

$$V(x,t) = \frac{FL^3}{EI} \delta_D, \tag{18}$$

where δ_D represents the "Influence Coefficient for Deflection".

Using (17) and (18) in (10) and rearranging,

$$Y(x,t) = \frac{FL^3}{EI} \left[\delta_D - \frac{c^4}{L^4} \sum_{n=1}^{\infty} \left\{ \frac{1}{K_n \lambda_n^4} F_n(t) \phi_n(x) \right\} \right], \tag{19}$$

where
$$\ddot{A}_n(t) = \frac{F}{\gamma L K_n} F_n(t). $$

From Eq. (9)

$$M(x,t) = -EI \frac{\partial^2 Y}{\partial x^2} = -EI \frac{\partial^2 V}{\partial x^2} - EI \frac{\partial^2 U}{\partial x^2}. \tag{20}$$

The quasi-static moment can be written down as

$$-EI \frac{\partial^2 V}{\partial x^2} = FL \delta_M, \tag{21}$$

where δ_M is the "Influence Coefficient for Moment".

Hence,
$$M(x,t) = FL \left[\delta_M + \frac{c^2}{L^2} \sum_{n=1}^{\infty} \left\{ \frac{1}{K_n \lambda_n^2} F_n(t) \bar{\phi}_n(x) \right\} \right], \tag{22}$$

where
$$\bar{\phi}_n(x) = \frac{c^2}{\lambda_n^2} \phi_n''(x). $$

Eq. (22) gives the bending moment at any section.

The "Amplification Factors for Deflection and Moment – (AFD and AFM)" are defined as

$$AFD = \frac{Y(x,t)}{\frac{FL^3}{EI}(\delta_D)_{maximum}} \tag{23}$$

and
$$AFM = \frac{M(x,t)}{FL(\delta_M)_{maximum}}. \tag{24}$$

$Y(x,t)$ and $M(x,t)$ are computed by using Eqs. (19) and (22) respectively. The influence coefficients and their maximum values are obtained by a static analysis of the structure.

2.3. Numerical Studies

Four bridges of different aspect ratios were selected for response calculations. Their dimensions were arrived at by approximating those of some of the existing bridges in North India [11]. The deflection and moment amplification factors and their maximum values were computed in each case for the critical cross section of the structure. The sections considered are:

Sections C and D   the mid-sections of the end spans MN and QR respectively.

Section S   the mid-section of the suspended span OP.

The two hinges O and P, and the intermediate support Section N (Fig. 1).

Table B. Some Salient Features of the Four Bridges

Bridge Type	Span lengths (meters)			Aspect ratios		Total Length of Bridge (meters)	EI (kg-m²)	γ (kg-sec²/ m²)	Funda- mental period (sec.)
	a	b	c	$\alpha=\dfrac{a}{c}$	$\beta=\dfrac{b}{c}$				
I	16.00	4.00	10.00	1.6	0.4	50.00	1523×10^6	556	0.130
II	18.24	1.14	11.40	1.6	0.1	50.16	1523×10^6	556	0.130
III	24.00	4.00	40.00	0.6	0.1	96.00	4554×10^6	944	0.487
IV	28.00	5.60	28.00	1.0	0.2	95.20	2674×10^6	876	0.415

Table B shows some salient features of the four bridges. The results of free vibration analysis required for the dynamic response calculations are taken from PAWHA [15].

The results of numerical studies are presented in two forms: 1. the Amplification Spectra, and 2. the "History Curves". The amplification spectra are the plots of any maximum response quantity against the speed parameter. The "Speed Parameter ξ" is defined by the relation $\xi = \dfrac{v T_1}{2L}$ where v is the speed of the moving force, T_1 the fundamental period of the bridge, and L the length of the bridge. A history curve for any response quantity shows the response as a function of time as the force moves along the bridge at a particular speed.

2.4. Discussion of Results

The time variation of the series $Y(x,t)$ and $M(x,t)$ in (19) and (22) has to be studied by selecting a suitable time interval. In this investigation, the time interval is taken to be one-tenth the lowest period of the bridge considered in the analysis.

The numerical results of the moving force problem, for various cases, are presented in Figs. 2 to 13. Fig. 2 shows the response history of bridge I under moving force, at the Section D, for a speed parameter of $\xi = 0.09$. The figure shows the influence of various modes on the response. It is clear that there is
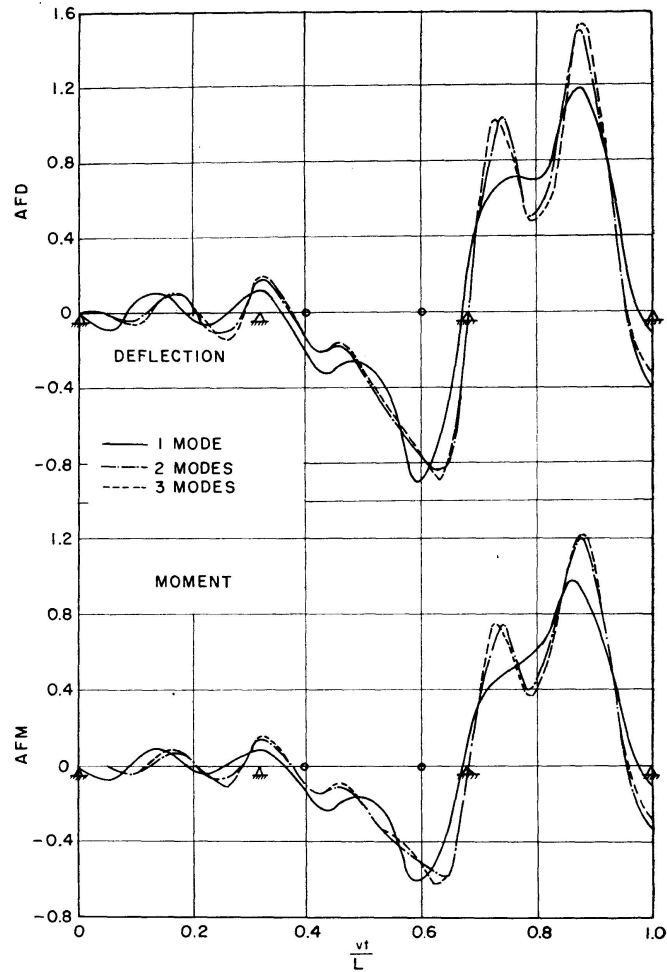
Fig. 2. Influence of various modes on the deflection and moment at section D, bridge I. $\alpha = 1.6$, $\beta = 0.4$, $\xi = 0.09$.
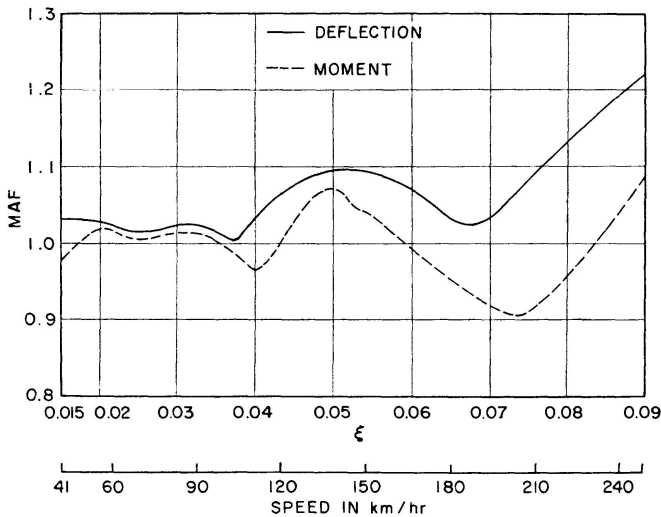

Fig. 3. Amplification spectra for the cantilever bridge I, section C. $\alpha = 1.6$, $\beta = 0.4$.

very little difference between the two-mode and three mode solutions. Similar history curves were obtained for bridges II, III and IV. It may therefore be inferred that the three mode solution is more than adequate for the moving force problem. Accordingly, only three modes have been considered in the following results.
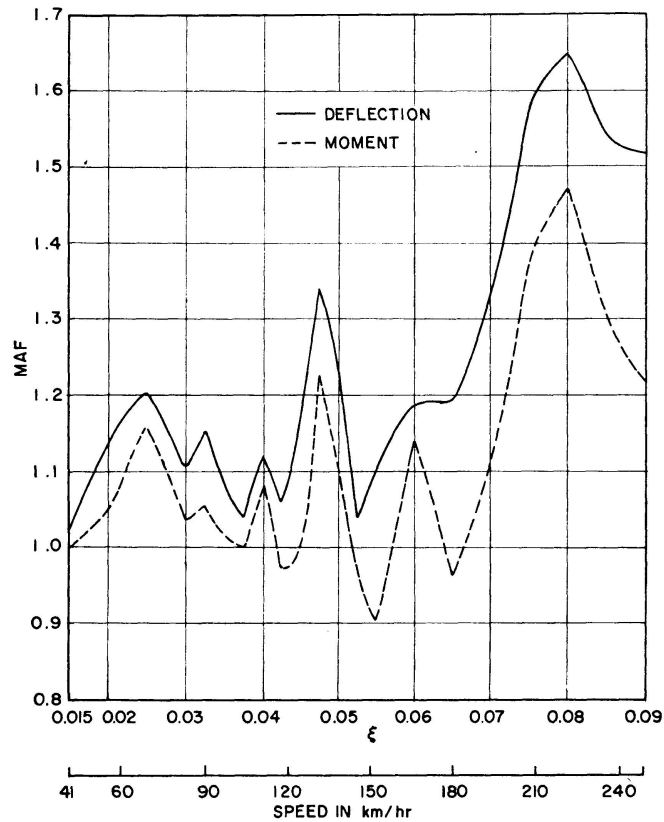
Fig. 4. Amplification spectra for the
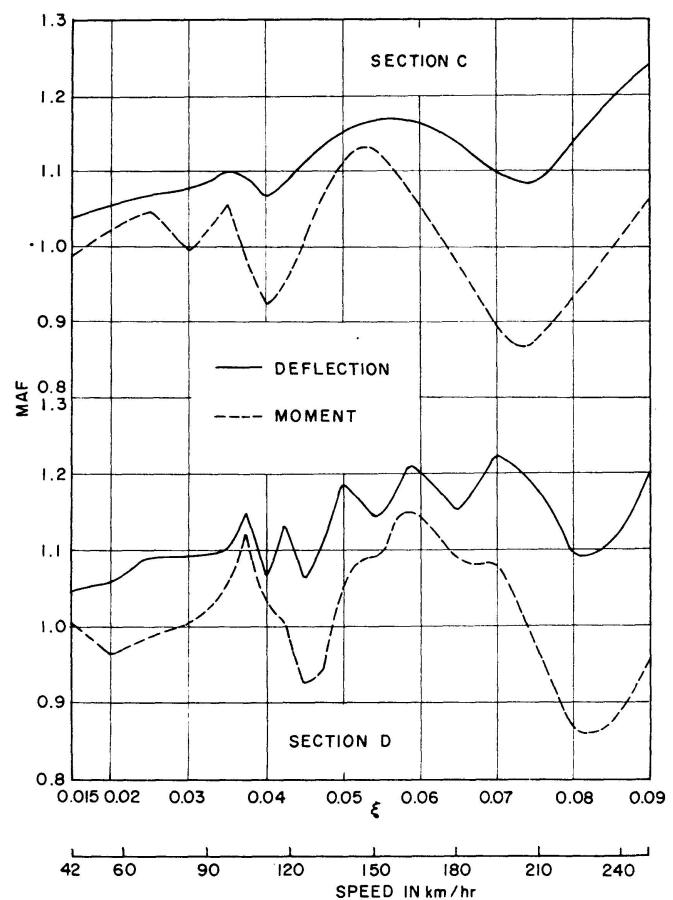cantilever bridge I, section D.
$\alpha = 1.6, \beta = 0.4.$

Fig. 5. Amplification spectra for the
cantilever bridge II, sections C and D.
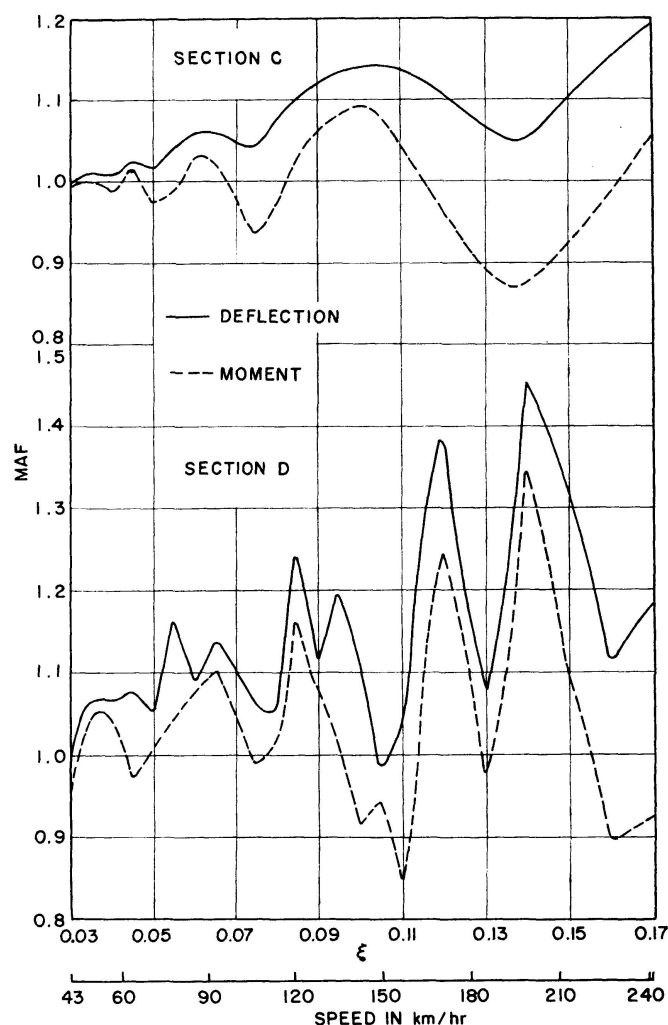$\alpha = 1.6, \beta = 0.1.$

Fig. 6. Amplification spectra for the cantilever bridge III, sections C and D. $\alpha = 0.6$, $\beta = 0.1$.

Figures 3 and 4 show the amplification spectra for bridge I, for the sections C and D respectively. It is clear that the section D experiences greater amplification as compared to section C, its counterpart on the left side. Figures 5 and 6 show the spectra for bridges II and III, at the same sections. The difference between the amplifications at C and D is not as pronounced in bridge II while it is significant in bridge III at the hinges O and P. The difference between the behaviour of the two hinges is seen to be quite large. In general it may be observed that while the force moves from left to right, the sections towards the right half the bridge are more susceptible to vibration than the sections on the left. It must be noted that this feature is not pronounced in bridge II which has a relatively stiff middle span and short cantilever arms. The presence of larger dynamic effects in the second half of the bridge has also been observed in the results of WEN and TORIDIS [8] and VELETSOS and HUANG [10].

Figures 8 to 11 show the typical response history curves for bridges I, II, III and IV of the section C. It is seen that the minimum dynamic response is attained when the moving force is close to the section C. The response
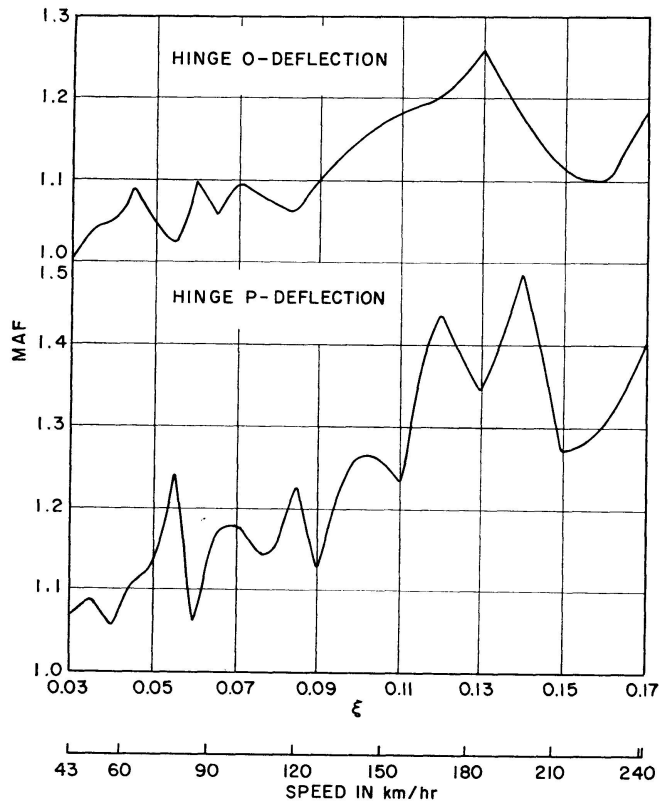
Fig. 7. Amplification spectra for the cantilever bridge III, sections O and P.
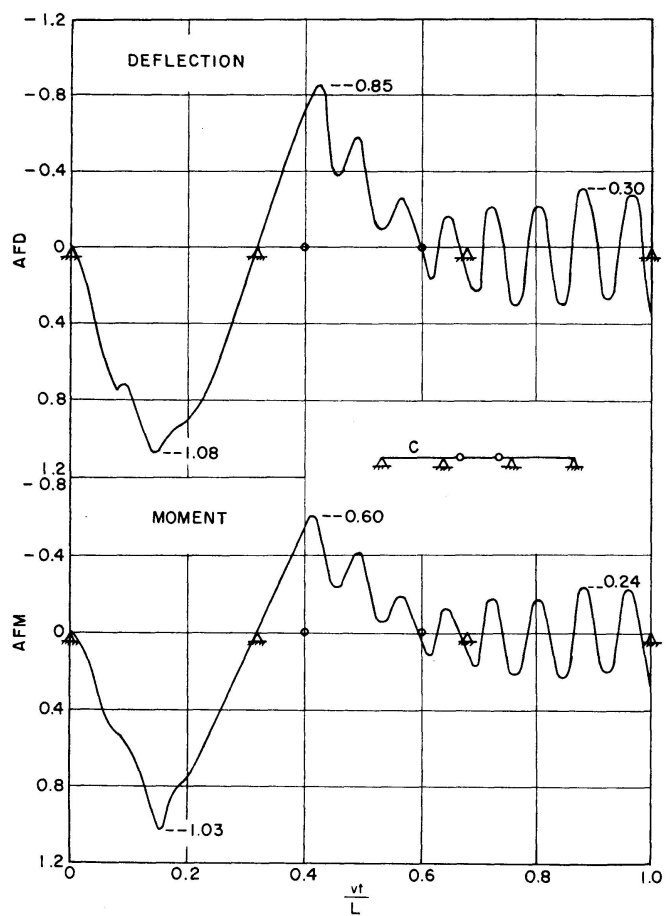$\alpha = 0.6$, $\beta = 0.1$.

Fig. 8. History curves for deflection and moment at C, bridge I.
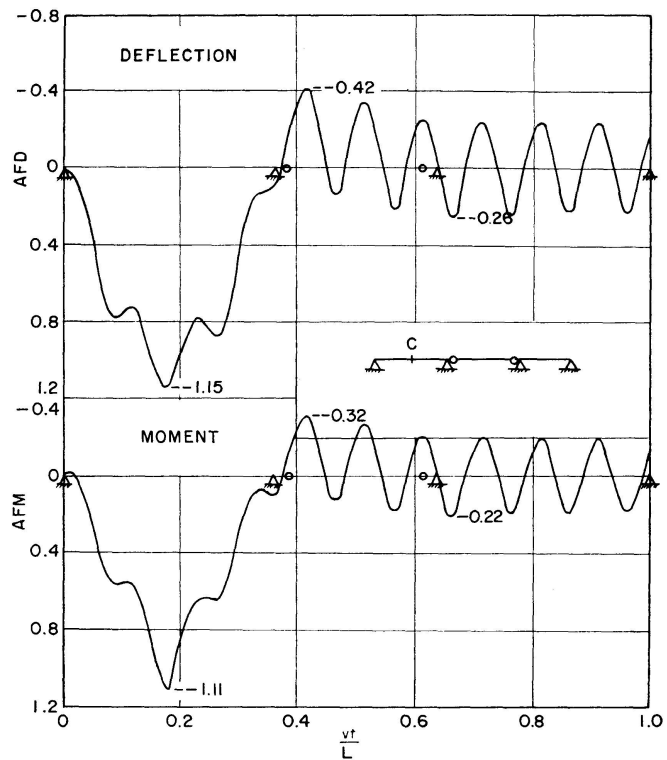$\alpha = 1.6$, $\beta = 0.4$, $\xi = 0.045$.

Fig. 9. History curves for deflection
and moment at C, bridge II.
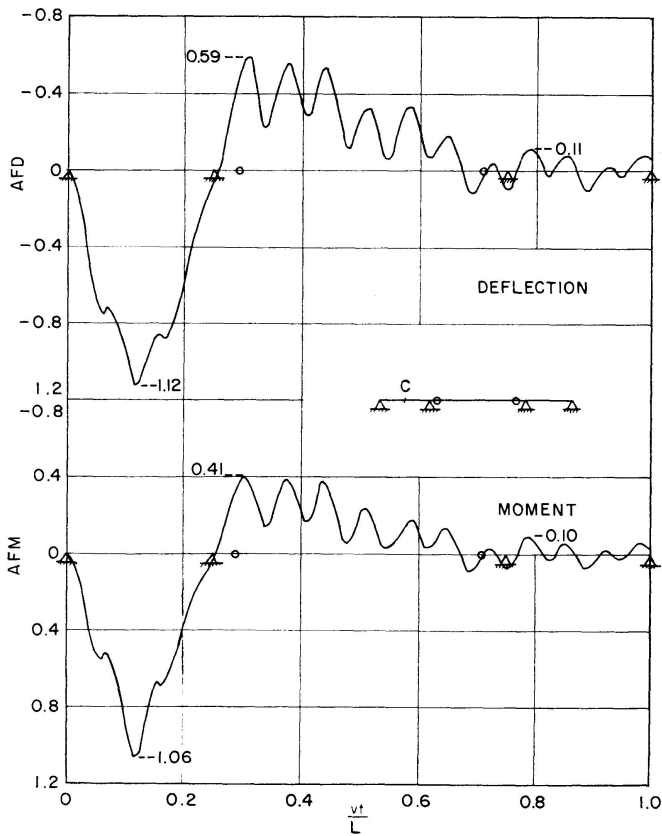$\alpha = 1.6$, $\beta = 0.1$, $\xi = 0.05$.

Fig. 10. History curves for deflection
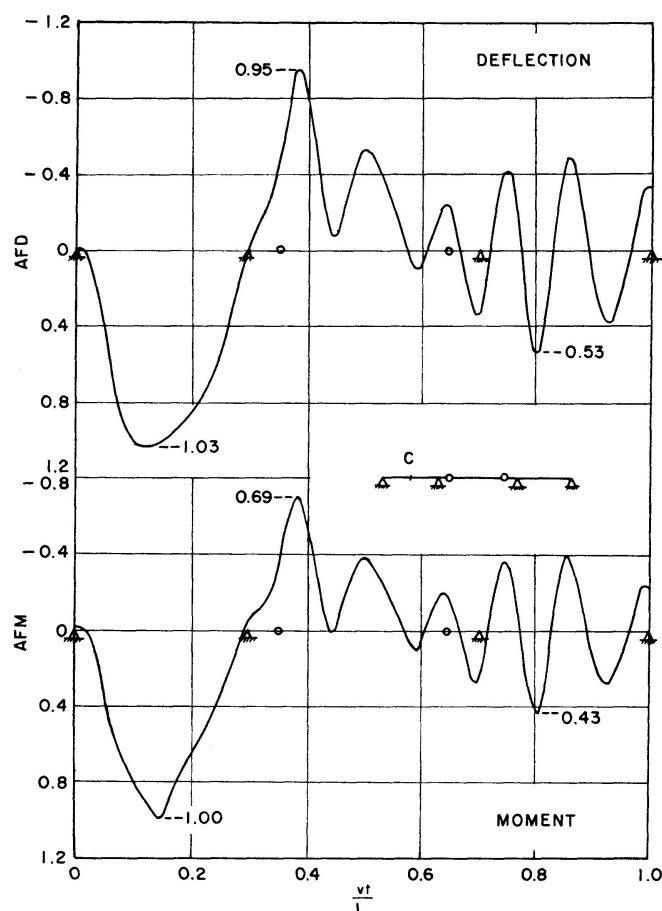and moment at C, bridge III.
$\alpha = 0.6$, $\beta = 0.1$, $\xi = 0.09$.

Fig. 11. History curves for deflection
and moment at C, bridge IV.
$\alpha = 1.0$, $\beta = 0.2$, $\xi = 0.08$.

decreases as the force moves on and a negative peak value is developed when the load is near the hinge. This negative peak value will be termed as the second maximum. For bridge I and IV the second maximum is comparable to the first maximum, while it is relatively smaller for bridge II and III. Another feature revealed by these figures is the persistence of oscillations even after the force crosses the second hinge P. The static response at C is zero for positions of the force right of P. But the inertia effect continues to be present owing to the energy input into the structure due to the passage of the moving force. This type of oscillation will be referred to as the "Residual oscillation". The figures show that bridges I, II and IV experience significant levels of residual oscillation. On the other hand, bridge III has very little of residual oscillation. This behaviour of the bridges may be examined in detail with reference to their structural properties. They are presented in Table C. It may be noted that the ratio of the second natural frequency to the fundamental is quite large for bridge III and it is close to unity for the other bridges. The table also shows that bridge III represents a combination of small values of α and β. In other words, short cantilever arms with relatively shorter anchor spans lead to low levels of residual oscillation.

Figure 12 shows a comparison of the maximum response in bridge I and a simply supported beam of the same flexural rigidity, whose span is $C + 2b$.

Table C. Frequency Ratios of the Four Bridges

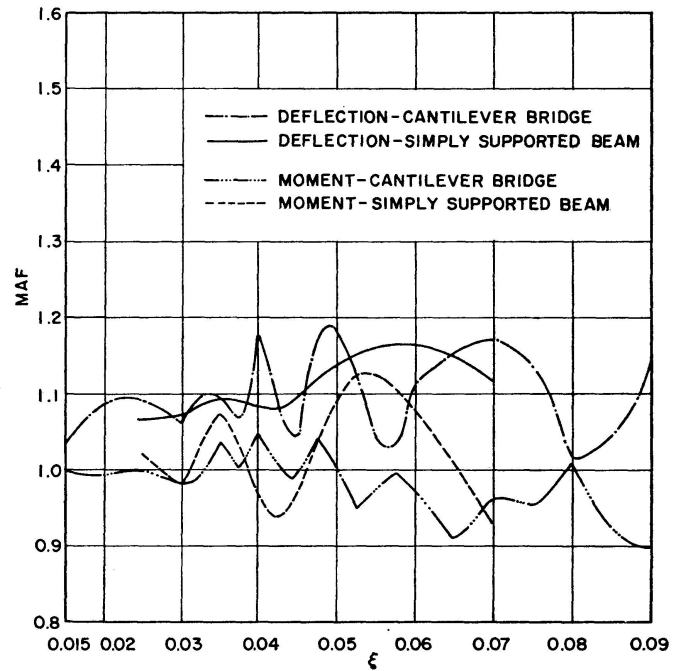| Bridge Type	Aspect Ratio $\alpha = \dfrac{a}{c}$	$\beta = \dfrac{b}{c}$	$\dfrac{\alpha}{\beta}$	Frequency (rad/sec) ω_1	ω_2	$\dfrac{\omega_2}{\omega_1}$
I	1.6	0.4	4	48.23	56.34	1.17
II	1.6	0.1	16	48.38	48.87	1.01
III	0.6	0.1	6	12.91	33.16	2.57
IV	1.0	0.2	5	15.13	19.90	1.31

Fig. 12. Comparison of maximum responses of the cantilever bridge I and the simply supported beam. Section at mid-span.
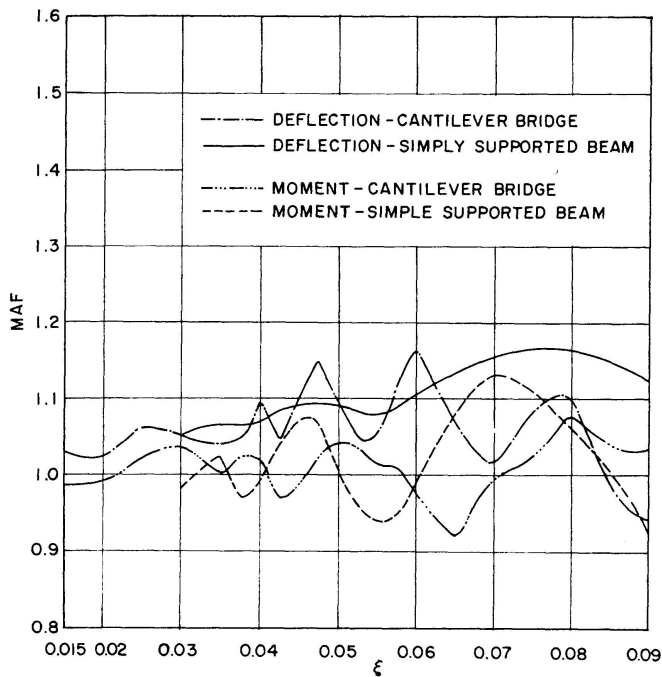

Fig. 13. Comparison of maximum responses of the cantilever bridge II and the simply supported beam. Section at mid-span.

The results for the simply supported beam are taken from JAGADISH [1]. The section S, at the midspan of the bridge is chosen for comparison with the midspan of the simply supported beam. It is seen that the deflection amplification of the cantilever bridge is more sensitive to variation in the speed parameter. The response is also higher. The moment amplification for the cantilever bridge, however, is not large and the beam theory furnishes conservative results. A similar trend is observed in bridge II as shown by Fig. 13.

3. Cantilever Bridge Under Moving Sprung Load

In this case the vehicle is treated as a mass-spring combination moving from left to right with a constant velocity. The damping in the vehicle is not considered. The multi-axle nature of the highway vehicle is disregarded in the following analysis. Owing to the assumptions, only a gross picture of the bridge vehicle behaviour may be obtained from the results presented in the following. The method of analysis adopted here follows a procedure similar to that of the moving force problem.

3.1. Analysis

A symmetrical double cantilever bridge under the passage of a moving sprung load is shown in Fig. 14. The moving load is assumed to traverse from left to right with a constant velocity v.
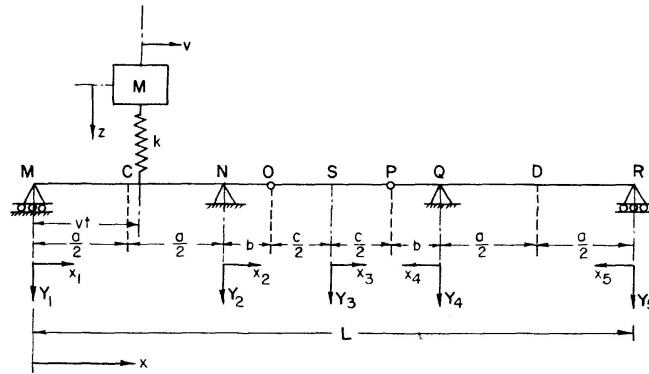
Fig. 14. Cantilever bridge under moving sprung load.

Ignoring damping, the equations of motion of the bridge-vehicle system are:

$$E I \frac{\partial^4 Y}{\partial x^4} + \gamma \frac{\partial^2 Y}{\partial t^2} = M (g - \ddot{z}) \delta (x - v t) \tag{25}$$

and

$$M \ddot{z} + K [z - Y (x, t)|_{x=vt}] = 0, \tag{26}$$

where Y represents the deflection of the bridge, EI, its flexural rigidity, γ, its mass per unit length; M is the mass of the moving load, z, its absolute deflec-

tion, and K, the stiffness of its spring. g represents the acceleration due to gravity, and $\delta(x - vt)$, the Dirac-delta function.

The solution of Eqs. (25) and (26) is obtained by expanding $Y(x,t)$ as

$$Y(x,t) = \sum_{n=1}^{\infty} A_n(t)\phi_n(x), \tag{27}$$

where $A_n(t)$'s are the normal co-ordinates and ϕ_n's, the characteristic shapes. $\phi_n(x)$ has already been defined in Table A.

Proceeding on similar lines as in the case of the moving force problem, the model equations are obtained as follows.

$$\ddot{A}_n(t) + \omega_n^2 A_n(t) = \frac{M(g - \ddot{z})\phi_n(vt)}{\gamma L K_n} \tag{28}$$

and
$$\ddot{z} + p^2 z = p^2 \sum_{n=1}^{\infty} A_n(t)\phi_n(vt). \tag{29}$$

Where $p^2 = \dfrac{K}{M}$ and represents the natural frequency of the sprung mass M,

and $K_n = \dfrac{1}{L} \int\limits_0^L \phi_n^2(x)\,dx$.

Eqs. (28) and (29) for the normal coordinates are solved on the computer by the Runge-Kutta-Nystrom procedure.

3.2. Deflection and Moment

The response $Y(x,t)$, as in the moving force problem, is conveniently split up into two parts $V(x,t)$ and $U(x,t)$ in order to achieve rapid convergence of the solution. The "quasi-static solution $V(x,t)$" represents the instantaneous static response due to the interaction force between the spring load and the beam as the load moves along the beam. The interaction force is determined from the solution of Eq. (29). $V(x,t)$ consists of the slowly converging component of the entire solution and is obtained by the elementary theory of bending of beams. The "Inertia Force solution $U(x,t)$" represents the dynamic response of the beam. As the inertia forces are well distributed throughout the structure convergence is rapid and a few terms would suffice.

Now
$$Y(x,t) = V(x,t) + U(x,t). \tag{30}$$

The final expressions for the deflection and moment reduce to

$$Y(x,t) = \frac{MgL^3}{EI}\left[\left(1 - \frac{\ddot{z}}{g}\right)\delta_D - \frac{\gamma L}{M}\frac{C^4}{L^4}\frac{1}{g}\sum_{n=1}^{\infty}\frac{1}{\lambda_n^4}\ddot{A}_n(t)\phi_n(x)\right], \tag{31}$$

$$M(x,t) = MgL\left[\left(1 - \frac{\ddot{z}}{g}\right)\delta_M + \frac{\gamma L}{M}\frac{C^2}{L^2}\frac{1}{g}\sum_{n=1}^{\infty}\frac{1}{\lambda_n^2}\ddot{A}_n(t)\bar{\phi}_n(x)\right], \tag{32}$$

where
$$\bar{\phi}_n(x) = \frac{C^2}{L^2}\phi_n''(x).$$

Amplification Factors

The amplification factors for deflection and moment $-AFD$ and AFM respectively, are expressed as:

$$AFD = \frac{Y(x,t)}{\dfrac{MgL^3}{EI}(\delta_D)_{max.}}$$ (33)

and $$AFM = \frac{M(x,t)}{MgL(\delta_M)_{max.}}.$$ (34)

Numerical Studies and Discussion of Results

Several parameters have to be considered while making a detailed study of the bridge-vehicle system. They are: 1. the speed parameter, 2. the mass ratio, 3. the frequency ratio, and 4. the initial oscillation of the sprung load.

The speed parameter ξ has the same meaning as in the moving force problem. In the results presented here, two values of the speed parameter — 0.09 and 0.045 are considered.

The mass ratio δ_1 is given by the relation $\delta_1 = (M/\gamma L)$. In this investigation, a mass ratio of 0.1 is taken throughout.
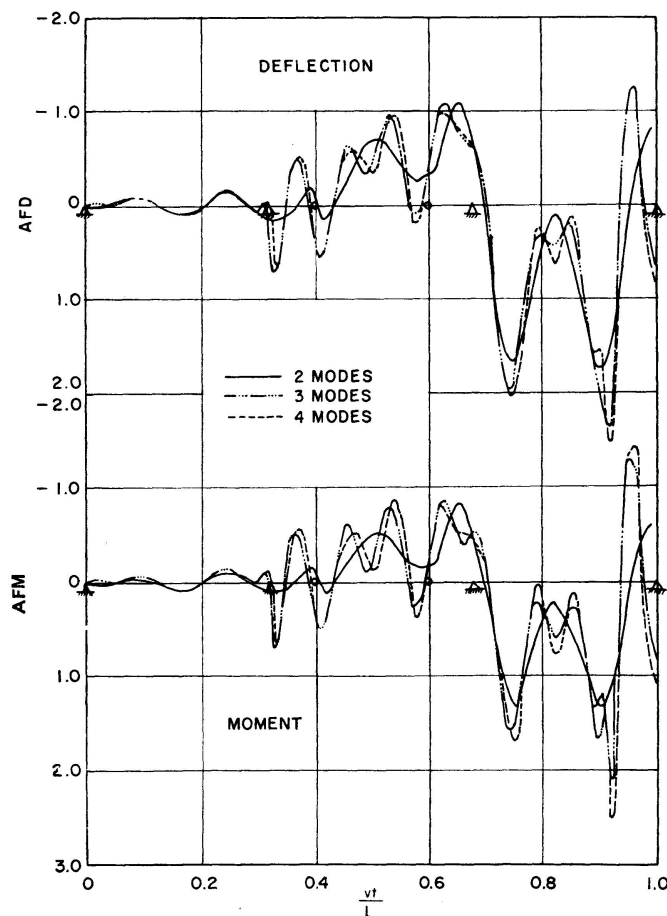

Fig. 15. Influence of various modes on the deflection and moment at section D, bridge I. $\alpha = 1.6$, $\beta = 0.4$, $\delta_1 = 0.1$, $\delta_2 = 0.2$, $\delta_3 = 0$, $\xi = 0.09$.
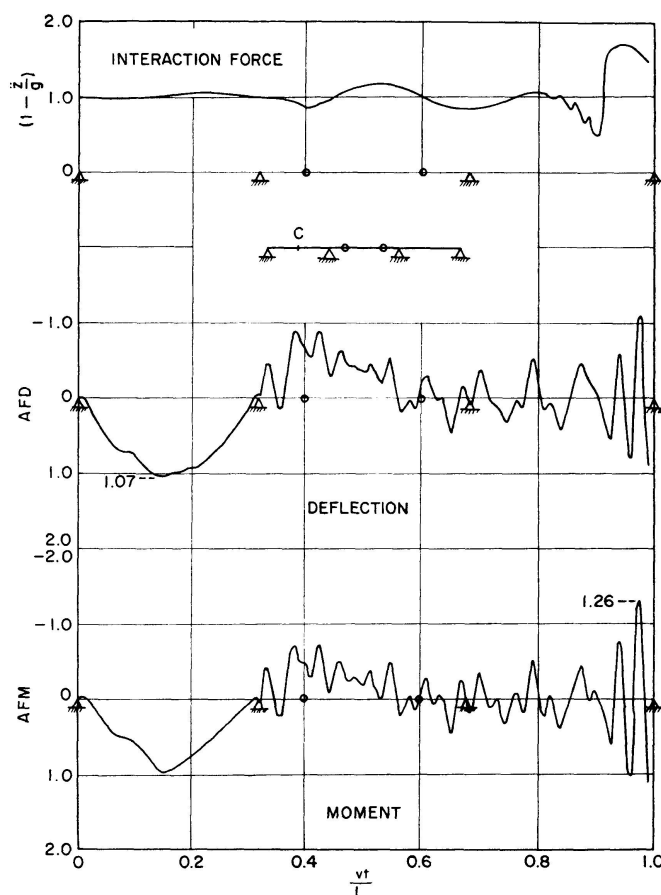
Fig. 16. History curves for interaction force, and deflection and moment at C, bridge I. $\alpha = 1.6$, $\beta = 0.4$, $\delta_1 = 0.1$, $\delta_2 = 0.3$, $\delta_3 = 0$, $\xi = 0.045$.

The frequency ratio δ_2 is given by the equation $\delta_2 = p/\omega_1$. The practical vehicle frequencies are usually less than the fundamental frequency of the bridge. In this case values of 0.2 and 0.3 for δ_2 are considered.

The initial oscillation of the vehicle can be described by its initial displacement and velocity. In the results presented here the initial velocity is taken to be zero. The initial displacement z, is expressed by the relation $z_0 = \delta_3 \left(\dfrac{M\,g}{k} \right)$ where $\dfrac{M\,g}{k}$ represents the static displacement of the sprung load. A value of 0.25 for δ_3 has been adopted here.

Fig. 15 represents the effects of various modes on the response of section D, bridge I. A maximum of four terms is taken in the series (31) and (32). The fundamental mode is not plotted as it obviously does not represent the correct solution. It is observed that the four-mode solution follows closely the three-mode solution, while the three-mode solution differs significantly from the two-mode solution. The four-mode solution, therefore, is considered in all the results that follow.

Figs. 16 and 17 show the time histories of response of sections C and D, bridge I. The speed parameter is 0.045 corresponding to a speed of 124.3 km/hr. The time interval selected for numerical integration is of the order of 1/35 of the period of the highest mode. It is observed in these figures that one of the
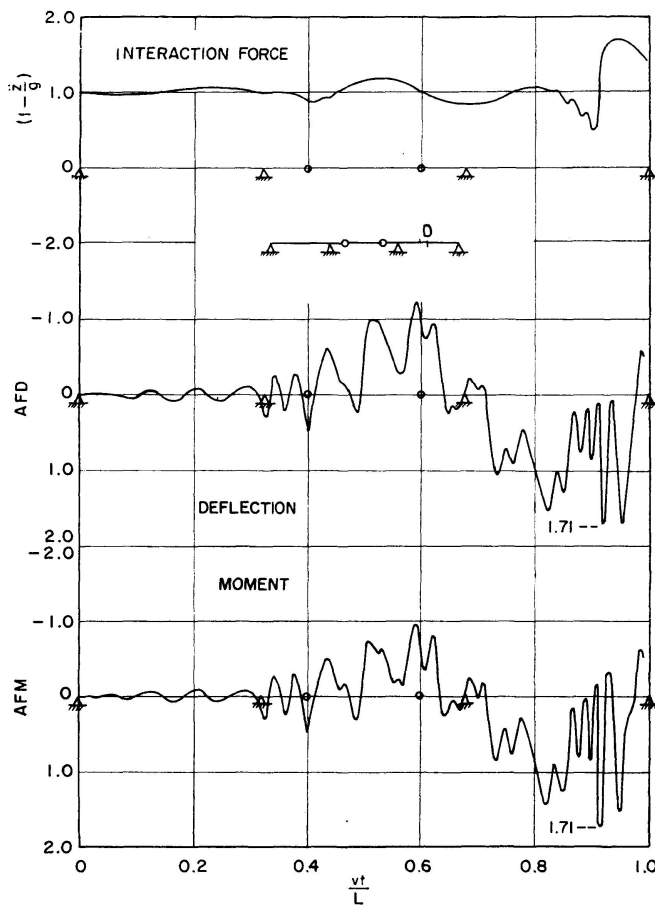
Fig. 17. History curves for interaction force, and deflection and moment at D, bridge I. $\alpha = 1.6$, $\beta = 0.4$, $\delta_1 = 0.1$, $\delta_2 = 0.3$, $\delta_3 = 0$, $\xi = 0.045$.

peak values of the response occurs close to the position of the maximum ordinate of the corresponding static influence line. The oscillations become more and more pronounced as the load approaches the right end. The variation of the interaction force as the load traverses along the bridge is also presented in the same figures. The interaction force R is given by the equation $R = Mg(1 - \ddot{z}/g)$. It is seen that the increased magnitude of the interaction force causes increased oscillations of the structure. It is also observed that as soon as the load crosses the intermediate support N, the third mode of the bridge is excited and continues to influence the response as long as the load is on the bridge. The moving load passes over a humped profile as it crosses the continuous support N. This leads to an impact effect, and the third mode of the bridge is excited. This feature of the excitation of the higher modes has also been observed by VELETSOS and HUANG [10]. It is also seen that a large amplification occurs as the sprung load is about to leave the bridge. This result must be viewed with some reservation since it might have been caused by the absence of damping in the vehicle and the bridge and the assumption of single axle loading. Detailed studies using more complex models for the vehicle are indicated in order to obtain accurate results.

4. Conclusions

Consideration of the first three modes is quite adequate while determining the response of the cantilever bridge to moving forces.

The response generally increases with increase in the value of the speed parameter. The force being assumed to move from left to right, the sections in the right half of the bridge are found to experience larger oscillations than the corresponding ones in the left half.

The maximum dynamic response is found to occur usually close to the position of the maximum ordinate of the corresponding static influence line.

The most critically stressed section generally happens to be the mid-point of the right end span, with the load moving from left to right.

The residual oscillations are minimum for cantilever bridges of comparatively larger suspended spans and shorter cantilevers and anchor spans.

For the moving sprung load case consideration of only three-modes does not seem to be adequate as there is significant deviation of the three-mode solution from the two-mode solution.

Excitation of higher modes takes place when the load passes over a humped profile on the bridge like any intermediate support and as such the higher modes influence the response in a significant way.

Notation

a	Length of the end span
b	Length of the cantilever span
c	Length of the suspended span
EI	Flexural rigidity of beam
g	Acceleration due to gravity
h	Time interval for numerical integration
j	Number of span
k	Stiffness of the spring
L	Total length of bridge
M	Mass of the moving sprung load
n	Number of mode
p	Circular frequency of the sprung load
R	Force of interaction between the bridge and the sprung load
T_1	Fundamental period of the bridge
t	Time
v	Speed of the moving force
x	Distance measured along the length of the bridge
Y	Deflection of bridge
z	Deflection of the sprung load

$A_n(t)$ Normal co-ordinate of the beam

$\left.\begin{array}{l} \alpha = \dfrac{a}{c} \\[2mm] \beta = \dfrac{b}{c} \end{array}\right\}$ Aspect ratios

γ Mass per unit length of the bridge

$\delta_1 = \dfrac{M}{\gamma L}$ Mass ratio

$\delta_2 = \dfrac{p}{\omega_1}$ Frequency ratio

δ_3 Initial oscillation parameter

δ_D Influence coefficient for deflection

δ_M Influence coefficient for moment

ω_n Circular frequency of bridge in the nth mode

λ_n Frequency parameter

$\xi = \dfrac{v T_1}{2 L}$ Speed parameter

$\phi_n(x)$ Characteristic shape function

$A\,F\,D$ Amplification factor for deflection

$A\,F\,M$ Amplification factor for moment

$M\,A\,F$ Maximum amplification factor

References

1. JAGADISH, K. S.: The Dynamic Response of Simple-Span Beam and Slab Bridges to Moving Loads. Thesis for the Ph. D. degree submitted to the Indian Institute of Science, Bangalore, 1968.
2. ORAN, C. and VELETSOS, A. S.: Analysis of Static and Dynamic Response of Simple Span, Multigirder Highway Bridges. Civil Engineering Studies, Structural Research Series No. 221, Univ. of Illinois, Urbana, 111, July 1961.
3. SUNDARA RAJA IYENGAR, K. T. and JAGADISH, K. S.: The Response of Beam and Slab Bridges to Moving Forces. Publ. IABSE, Vol. 28–II, 1968.
4. SUNDARA RAJA IYENGAR, K. T. and JAGADISH, K. S.: The Dynamic Response of Highway Bridges. Publ. IABSE, Vol. 30–II, 1970.
5. OEHLER, L. T.: Vibration Susceptibilities of various Highway Bridge Types. Journal of the Structural Division, ASCE, Vol. 83, No. ST 4, Proc. Paper 1318, July 1957.
6. KONISHI, I. and KOMATSU, S.: Vibration Behaviour of Gerber Beam. Technical Report, Vol. 6, No. 3. The Engineering Research Institute, Kyoto University, Kyoto, Japan, February 1956.
7. HUANG, T. and VELETSOS, A. S.: A Study of Dynamic Response of Cantilever Highway Bridges. Civil Engineering Studies, Structural Research Series No. 206, Univ. of Illinois, Urbana, III, October 1960.
8. WEN, R. K. and TORIDIS, T.: Dynamic Behaviour of Cantilever Bridges. Journal of the Engineering Mechanics Division, ASCE, Vol. 88, No. EM 4, Proc. Paper 3229, August 1962.
9. JAGADISH, K. S. and PAHWA, J. L.: The Vibration of Cantilever Bridges. J. Sound Vib. (1968) 7 (3), 449–459.

10. VELETSOS, A. S. and HUANG, T.: Analysis of Dynamic Response of Highway Bridges. Journal of the Engineering Mechanics Division, ASCE, Vol. 96, No. EM 5, Proc. October 1970.
11. SINHA, S. N., PRASAD, B. and PRASAD, P. J.: Analytical Study of Some Bridge Articulation Failure. Paper No. 231. Indian Roads Congress, November 1961.
12. KATAYAMA, T.: A Review of Theoretical and Experimental Investigations of Damping in Structures. UNICIV REPORT, 1–4, July 1965 (University of New South Wales, Kensington, N.S.W., Australia).
13. WALKER, W. H. and VELETSOS, A. S.: Dynamic Response of Simple-Span Highway Bridges to Moving Vehicles. Engineering Experiment Station, Bulletin No. 486, Univ. of Illinois, Urbana, III, 1966.
14. NAGARAJU, N.: The Dynamic Response of Cantilever Bridges to Moving Loads. Thesis submitted for the M. Sc. degree in the Faculty of Engineering, Indian Institute of Science, Bangalore, January 1971.
15. PAHWA, J. L.: The Free Vibrations of Double Cantilever Bridges. Dissertation submitted for the M. E. degree in Civil Engineering, Indian Institute of Science, Bangalore, 1967.

Summary

The dynamic behaviour of double cantilever bridges is studied under moving loads. The bridge is treated as a beam and the vehicle is represented by two simple models: 1. a moving constant force, 2. a moving sprung force. Detailed numerical results are presented for four bridges of different aspect ratios for the moving force problem and for a few typical cases in the moving sprung load problem. The results of numerical studies are presented in two forms: 1. the Amplification Spectra and 2. the "History Curves".

Résumé

Le comportement dynamique de ponts en poutres articulées est étudié sous l'influence de charges mouvantes. Le pont est traité comme poutre et le véhicule est représenté par deux modèles simples: 1. une force mouvante et constante, 2. une force mouvante sur ressorts. Des résultats numériques détaillés sont présentés pour quatre ponts de différents rapports de longueurs traitant du problème de forces mouvantes et pour quelques cas typiques du problème de forces sur ressorts. Les résultats des études numériques sont présentés sous deux aspects: 1. Régime d'amplification et 2. courbes de conformité.

Zusammenfassung

Das dynamische Verhalten von Gerberträgerbrücken wird unter dem Einfluss bewegter Lasten untersucht. Die Brücke wird als Balken betrachtet und das Fahrzeug durch zwei einfache Modelle dargestellt: 1. eine konstant wirkende bewegte Kraft, 2. eine bewegte federnde Kraft. Numerische Einzelresultate werden für vier Brücken mit verschiedenem Längenverhältnis für das Problem bewegter Kräfte und für einige typische Fälle des gefederten Lastproblems vorgelegt. Die Ergebnisse der numerischen Untersuchungen werden unter zwei Gesichtspunkten geliefert: 1. Verstärkungseinflüsse und 2. Gesetzmässigkeitskurven.